Synthesis of Automatic Control System of Traction Asynchronous Motor of Transport Diesel-Generator Power Plant

¹Kulagin D., ²Maslov I.

¹National University "Zaporizhzhya Polytechnic" Zaporizhzhya, Ukraine ² Dunai Institute of National University "Odessa Maritime Academy" Izmail, Ukraine

Abstract. This paper presents the synthesis of an automatic control system for a traction induction motor used in a transport diesel-generator power plant. The objective of the study is to improve the stability and dynamic performance of current regulation under varying operating conditions. The research covers three main aspects: analysis of the diesel-generator plant as a control object, development of a methodology for designing current regulators, and validation of the synthesized regulators against real transient processes. The proposed methodology provides a systematic approach to constructing structural schemes of the current control loop and the closed-loop system. A new regulator transfer function is synthesized based on transient performance criteria, specifically limiting settling time and overshoot, while maintaining robustness to parameter variations caused by ambient temperature. Analysis shows that the fastest current regulation loop, which determines the system's overall dynamics, becomes unstable when a conventional regulator based on subordinate control is applied. In practice, widely used serial diesel-generator plants exhibit temperature-induced variations in stator resistance during warm-up, leading to significant overshoot and reduced responsiveness. These effects highlight the limited robustness of existing regulator designs. In contrast, the newly synthesized regulator demonstrates stable transient responses even under resistance variations, confirming its adaptability and efficiency in real conditions. The results provide a foundation for the development of modern control systems for transport diesel-generator power plants, ensuring stable operation, required dynamic properties, and improved reliability. Consequently, the findings have practical significance for creating next-generation traction drive control systems for railway and other transport applications.

Keywords: power plant, automatic control, autonomous voltage inverter, electrical apparatus, electrical machines, mathematical modelling, electrical systems and networks.

DOI: https://doi.org/10.52254/1857-0070.2025.4-68.02

UDC: 621.31: 621.436:629.5:656

Sinteza sistemului de control automat al motorului asincron de tracțiune al centralei electrice cu motor diesel pentru transport 1 Kulagin D., 2 Maslov I.

¹Universitatea Națională "Politehnica din Zaporizhzhya", Zaporizhzhya, Ucraina ²Institutul Dunai al Universității Naționale "Academia Maritimă din Odesa", Izmail, Ucraina Rezumat: Această lucrare prezintă sinteza unui sistem de control automat pentru un motor cu inducție de tracțiune utilizat într-o centrală electrică diesel-generator pentru transport. Obiectivul studiului este de a îmbunătăți stabilitatea și performanța dinamică a reglării curentului în condiții variabile de funcționare. Cercetarea acoperă trei aspecte principale: analiza centralei diesel-generator ca obiect de control, dezvoltarea unei metodologii pentru proiectarea regulatoarelor de curent și validarea regulatoarelor sintetizate în raport cu procesele tranzitorii reale. Metodologia propusă oferă o abordare sistematică pentru construirea schemelor structurale ale buclei de control al curentului și ale sistemului în buclă închisă. O nouă funcție de transfer a regulatorului este sintetizată pe baza unor criterii de performanță tranzitorie, limitând în mod specific timpul de stabilizare si depăsirea, mentinând în acelasi timp robustetea la variatiile parametrilor cauzate de temperatura ambiantă. Analiza arată că cea mai rapidă buclă de reglare a curentului, care determină dinamica generală a sistemului, devine instabilă atunci când se aplică un regulator convențional bazat pe control subordonat. În practică, centralele diesel-generatoare de serie utilizate pe scară largă prezintă variații induse de temperatură ale rezistenței statorice în timpul încălzirii, ceea ce duce la depășiri semnificative și la o capacitate de răspuns redusă. Aceste efecte evidențiază robustețea limitată a proiectelor de regulatoare existente. În schimb, regulatorul nou sintetizat demonstrează răspunsuri tranzitorii stabile chiar și la variații de rezistență, confirmând adaptabilitatea și eficiența sa în condiții reale. Rezultatele oferă o bază pentru dezvoltarea unor sisteme moderne

© Kulagin D., Maslov I. 2025

PROBLEMELE ENERGETICII REGIONALE 4 (68) 2025

de control pentru centralele electrice cu generatoare diesel pentru transport, asigurând o funcționare stabilă, proprietățile dinamice necesare și o fiabilitate îmbunătățită.

Cuvinte-cheie: centrală electrică, control automat, invertor autonom de tensiune, aparatură electrică, mașini electrice, modelare matematică, sisteme și rețele electrice.

Синтез системы автоматического управления тяговым асинхронным двигателем транспортной дизель-генераторной энергетической установки ¹Кулагин Д.А., ²Маслов И.З.

¹Национальный университет «Запорожская политехника», Запорожье, Украина

²Дунайский институт Национального университета «Одесская морская академия», Измаил, Украина Аннотация. Основная цель исследования — синтез системы автоматического управления тяговым асинхронным двигателем транспортной дизель-генераторной энергетической установки. Для достижения поставленной цели были решены следующие задачи: анализ транспортной дизель-генераторной энергетической установки как объекта управления тяговым асинхронным двигателем, разработка методики синтеза регуляторов тока системы автоматического управления асинхронным двигателем и проверка соответствия полученных результатов реальным переходным процессам. Наиболее важными результатами являются получение структурных схем контура регулирования тока и замкнутой системы, а также синтез передаточной функции нового регулятора по критерию обеспечения требуемых характеристик переходного процесса (ограничение времени переходного процесса и показателя колебательности) при наличии изменения параметров объекта регулирования под влиянием температуры окружающей среды. Исследование показало, что самый быстродействующий контур регулирования тока, определяющий динамические свойства всей системы, при использовании базового регулятора, синтезированного методом подчиненного регулирования, демонстрирует нестабильные переходные характеристики. В частности, для известных серийных дизель-генераторных транспортных энергоустановок, при изменении сопротивления статорной цепи под влиянием температурных колебаний в процессе прогрева энергоустановки возникает значительное перерегулирование, что приводит к уменьшению быстродействия регуляторов. Это свидетельствует о нестабильности работы таких регуляторов при вариации параметров объекта. В отличие от этого, полученные переходные характеристики нового синтезированного регулятора тока подтверждают стабильность его работы даже при изменении активного сопротивления статорной цепи, что доказывает его лучшую адаптивность и эффективность в реальных условиях. Результаты исследования позволяют проводить разработку современных систем управления дизель-генераторными энергетическими установками транспортных средств, обеспечивая при этом стабильность и требуемые системные свойства в условиях эксплуатации. Значимость полученных результатов состоит в практическом приложении, поскольку они способствуют созданию более надежных, эффективных и адаптивных систем управления для транспортных средств. Ключевые слова: энергетическая установка, автоматическое управление, автономный инвертор

напряжения, электрические аппараты, электрические машины, математическое моделирование, электрические системы и сети.

INTRODUCTION

A considerable body of research [1-4] is dedicated to establishing the scientific foundations for the technical operation of transport energy system components. Several studies [5-8] emphasize the mutual interactions between subsystems and their aggregates particularly combined configurations such as converter-motor assemblies, motor-drive units, and diesel-generator sets — and their impact on the overall energy efficiency of the drive system. Practical experience in the operation of transport energy systems [9-12] demonstrates that their energy-saving potential is inherently more complex than that of isolated subsystem groups. Consequently, it is essential to investigate transport energy systems not only at the level of individual components, but also with regard to the emergent interdependencies that determine

total energy consumption [13, 14]. Enhancing the energy efficiency of such systems requires a comprehensive approach — optimizing the operating regime of the system as a whole, ensuring the rational performance of its components, and exploiting the energy-saving potential arising from their functional interrelationships.

Neglecting this principle in practice leads to situations where the energy-efficient operation of individual units of the power plant, or their optimal control from the standpoint of energy performance, does not guarantee the effective functioning of the system as a whole. As a consequence, this results in increased fuel consumption [15, 16]. Similarly, operating the diesel engine within its economic performance range often induces non-optimal behavior of other elements of the power plant, preventing them from realizing their maximum energy-saving potential [17, 18].

The application of an integrated approach to power system control — whereby the system as a whole operates in the most energy-efficient regime achievable while meeting technical performance requirements, and each subsystem functions in a mode that maximizes the overall energy potential of the system — enables the full realization of the energy-saving potential of the entire drive installation [19, 20].

Such an approach can be implemented by accounting for the synergistic properties of the power system, whereby the operating regimes of the thermal engine, synchronous generator, frequency converter, auxiliary power system, and drive motor are selected not with regard to their individual energy potential, but with the objective of maximizing the energy potential of the system as an inseparable whole. In this context, addressing the energy-efficiency requirements of individual components is necessary only insofar as it ensures the realization of the overall energy potential of the entire power system.

The development of a control system that exhibits low sensitivity to parameter variations of the controlled plant — an inherent characteristic of transport power systems during operation — can be achieved on the basis of regulators synthesized using the polynomial method [21, 22]. The application of such regulators in electric drive systems has been validated and substantiated with respect to the resulting transient characteristics [23, 24]. At the same time, the problem of reducing the dependence on plant parameter variations through the synthesis of automatic control system regulators and the optimal design of such regulators remains highly relevant and has been addressed by numerous researchers [25, 26]. However, the synthesis of control system elements for a traction asynchronous motor within a transport diesel-generator power plant has not yet been comprehensively investigated.

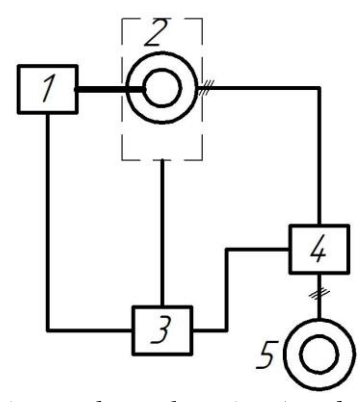
A critical issue is the analysis of the performance of synthesized control regulators under parameter variations, a feature particularly pronounced in transport power installations. Consequently, the topic of this study is of

significant relevance. The objective of this work is the synthesis of automatic control system elements for the traction asynchronous motor of a transport diesel—generator power plant.

To achieve this objective, it is necessary to transport diesel-generator analyze the installation, develop a methodology synthesizing the automatic control system elements for the traction asynchronous motor, and validate the adequacy and consistency of the obtained results with real transient processes. The synthesis of the transfer function of the new regulator will be carried out according to the criterion of ensuring the required transient process characteristics — specifically, limiting the transient time and overshoot factor — under conditions of parameter variations in the controlled plant caused by ambient temperature effects.

I. RESEARCH METHODS

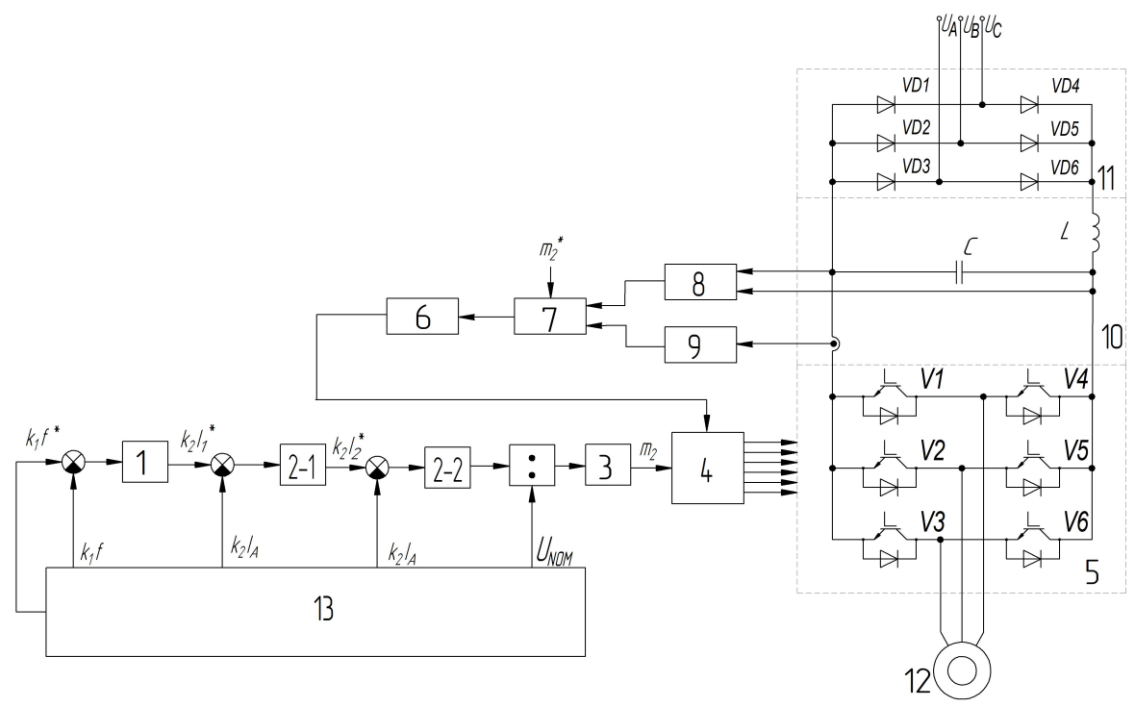
The power system, whose structural diagram is presented in Fig. 1, functions as a combined power source for the drive installation and the general onboard electrical consumers.



1 — primary thermal engine (predominantly diesel); 2 — synchronous generator (the dashed line indicates the synchronous generator—exciter system); 3 — automatic control system; 4 — traction converter; 5 — asynchronous machine.

Fig. 1. Structural diagram of the transport power system (illustrated for a single circuit).

The corresponding structural diagram of the control system for the traction asynchronous motor of the transport diesel–generator power plant is shown in Fig. 2.



1- frequency regulator; 2-1- first current regulator; 2-2- second current regulator; 3- signal limitation unit; 4- autonomous inverter control system; 5- autonomous voltage inverter; 6- reference generator; 7- electromotive force sensor; 8- voltage sensor; 9- active current sensor; 10- filter unit; 11- rectifier; 12- asynchronous motor; 13- centralized information and measurement system.

Fig. 2. Structural diagram of the automatic control system for the traction asynchronous motor of the transport diesel–generator power plant.

Strict market requirements necessitate the development of frequency converters for AC asynchronous drives with improved technical and economic performance, specifically with respect to meeting the required transient response characteristics. The conducted studies indicate the need to modernize asynchronous drive control systems by enhancing regulator parameters and implementing new control algorithms.

During the development of the automatic frequency control system for the asynchronous drive, the feasibility of applying the primary control principles — amplitude, vector, and quasi-vector — was analyzed. A comparison of the advantages and limitations of these approaches led to the conclusion that optimal control can be achieved by directly influencing the frequency and amplitude of the fundamental harmonic components of currents and voltages, while phase control should be implemented through additional modulation of the frequency control channel. Consequently, a combined control principle was adopted, integrating pulsewidth modulation (PWM), amplitude, and twozone control. This approach is currently considered promising due to its significant economic and technical advantages in the design of drive systems.

According to recommendations [27, 28], in the low-output-voltage regulation zone, the PWM control principle should be applied, as this type of control eliminates the discrete rotation of the motor shaft, which can occur, for example, under amplitude control. Therefore, during motion phases with maximum acceleration, while maintaining constant wheel-rail adhesion at low speeds, the use of PWM control is most appropriate [29, 30]. Consequently, when a motion command is issued by the drive control system, the generation of control pulses for the inverter switches should be performed according to the PWM principle.

Based on an analysis of frequency drive control principles [31, 32], it can be concluded that the most economically efficient control is achieved following the Kostenko law. That is, after exiting the low-output-frequency regulation zone, PWM control alone cannot provide the most economically advantageous system operation, as can be achieved under the Kostenko law.

Thus, when the output voltage of the autonomous voltage inverter (AVI) reaches the nominal operating voltage of the auxiliary power system, the generation of control signals for the AVI switches should be performed according to the amplitude control principle. In this mode, the traction power installations operate until the DC bus reaches the nominal operating voltage of the traction power system. During this period, motion occurs with increasing power draw from the diesel engine and a corresponding rise in speed. Subsequently, depending on the speed command from the information-control system — i.e., when operating in the zone of maximum diesel power extraction and the need for further speed increase — the control system transitions to the weakened flux linkage control zone. The reduction of the rotor flux linkage vector magnitude is achieved at a constant AVI output voltage by further increasing the frequency reference for the traction motor. The adjustment of the rotor flux linkage vector magnitude is performed proportionally based modulation signal.

A distinctive feature of the developed system is its rotor-speed-based partitioning, i.e., the absence of a mechanical speed sensor, where vector orientation relies on the electromotive force (EMF) of the motor, measured indirectly through active current and effective voltage sensors in the DC link.

The transfer functions of the frequency regulators, corresponding to the tuning of the frequency control loops at the modular and symmetric optimum, are defined by the expressions [33-35]:

$$W_{I}(p) = \frac{k_2 \cdot J}{4 \cdot T_m \cdot \Psi_r \cdot k_I \cdot k_r} \tag{1}$$

$$W_2(p) = \frac{(8 \cdot T_m \cdot p + 1) \cdot k_2 \cdot J}{32 \cdot T^2_m \cdot \Psi_n \cdot k_1 \cdot k_2 \cdot p}.$$
 (2)

where k_1 and k_2 — frequency- and current-dependent gain coefficients; $T\mu$ — rectifier time constant; J — equivalent drive moment of inertia; p — Laplace operator; ψ_r — rotor flux linkage vector magnitude.

Since the internal coupling through the EMF degrades the quality of the motor current and speed control, it becomes necessary to compensate for it. The influence of the EMF in the system is significantly greater compared to

DC systems, and compensating for the motor's rotational EMF allows the autonomous inverter system to be linearized and, in most cases, the motor couplings to be neglected. The transfer functions of the current regulators, synthesized using the subordinate control method, are expressed as follows:

$$W_{2-1}(p) = \frac{1}{4 \cdot T_m} \tag{3}$$

$$W_{2-2}(p) = \frac{k}{T_s \cdot p + I} \tag{4}$$

where T_s — stator winding time constant; k — coefficient accounting for the inverter commutation function magnitude, filter resistances, controlled plant parameters, and the voltage transfer ratio of the power electronic converter.

Since the fastest-acting control loop in the automatic control system of the traction asynchronous motor of the transport diesel—generator power plant is the current regulation loop, which determines the dynamic properties of the entire system, there is an evident need to improve the traction drive system and enhance operational efficiency (including improving dynamic parameters and achieving standardized transient characteristics of the energy circuits and control systems).

To increase operational efficiency, it is necessary to employ control system design and synthesis methods that provide high dynamic performance, robustness to disturbances, and resilience to parameter variations in the loops during operation, which is especially relevant for transport systems operating under rapid changes in temperature, load, and corresponding energy circuit parameters. The polynomial method, used for the synthesis of regulators and control system structures, meets these requirements and provides more stable performance of the controlled plant compared to traditional design approaches. The use of this method is promising for optimizing and improving traction, dynamic, and energy performance.

We proceed to synthesize the second current regulator for such a loop, as it determines the quality of the transient response. The closed-loop current control system of the asynchronous motor can be represented as a series connection of the controlled plant and the corresponding regulator, enclosed within a feedback loop.

The asynchronous motor is a nonlinear, highorder system. Its behavior is described by a complex system of differential equations that are difficult to solve analytically. Transitioning to a transfer function, expressed as a ratio of polynomials, allows the use of classical automatic control theory, simplifying the development of regulators [36-38]. Based on the transfer function, the regulator parameters can be readily calculated [39].

For synthesizing the current regulator, the transfer function of the controlled plant should be expressed as follows [40, 41]:

$$W_{ob}(p) = \frac{P(p)}{Q(p)} = \frac{k_0 \cdot P_{k+}(p) \cdot P_{n+}(p) \cdot P_{-}(p)}{Q_{k+}(p) \cdot Q_{n+}(p) \cdot Q_{-}(p) \cdot p^s}, (5)$$

where the polynomials P.(p) and Q.(p) respectively contain the right-hand and neutral zeros and poles of the controlled plant, excluding those located at p = 0;

The polynomials $P_{n+}(p)$ and $Q_{n+}(p)$ respectively contain only those left-hand zeros and poles of the controlled plant that are not compensated;

the polynomials $P_{k+}(p)$ and $Q_{k+}(p)$ respectively have as their zeros only the left-hand zeros and poles of the controlled plant that are compensated by the regulator;

the coefficient s takes values of 0, 1, or 2, corresponding to the number of poles of the plant at p = 0;

the coefficient k_0 is the gain factor of the controlled plant loop.

Considering that the compensation of the polynomials results in the cancellation of certain poles or zeros of the controlled plant, and given that not all zeros and poles should be compensated (compensating $P_{-}(p)$ and $Q_{-}(p)$ would compromise system stability), the transfer function of the current regulator, which ensures satisfactory system accuracy and dynamic performance, is expressed as follows:

$$W_{cr}(p) = \frac{(Tp+1)(r_1p+r_0)}{(v_1p+v_0)pk}.$$
 (6)

where r is the satisfactory order of astatism;

R(p) and V(p) are the corresponding polynomials formed during the synthesis of the current regulator.

To determine the regulator coefficients, the values from equations (5) and (6) must be

substituted into the polynomial synthesis expression:

$$R(p) \cdot P_{-}(p) \cdot P_{n+}(p) + V(p) \cdot Q_{-}(p) \cdot Q_{n+}(p) \cdot p^{r} =$$

$$= H(p),$$

$$(7)$$

where H(p) — The characteristic polynomial of the closed-loop system, whose coefficients are determined to satisfy the required transient response shape and decay time, corresponds to one of the well-known standard distributions (Newton's binomial, Butterworth, Bessel, Chebyshev, or the integral performance indices I_2 and I_3). The commonly used expressions for the coefficients of the characteristic polynomial are widely applied in practice depending on the desired transient response specifications.

Solving equation (7) provides expressions for the unknown polynomials R(p) and V(p), which are required to compute the transfer function of the regulator (6).

The solution of equation (7) is proposed to be carried out using the method of undetermined coefficients, due to the relative simplicity of implementing this approach in dynamic applications.

The minimal solution of the polynomial equations corresponds to the lowest degrees of the polynomials R(p) and V(p), respectively, and allows the establishment of the minimal order of the current regulator transfer function (6). This approach contributes to achieving high-speed performance of the closed-loop current control system by selecting the minimal degree for the characteristic polynomial of the closed-loop current control system.

Let us introduce a general conditional expression: let |X| denote the degree of an arbitrary polynomial X(p). This allows us to express the minimal degrees of the polynomials in expression (7) as follows:

$$|R| = |Q_{-}| + |Q_{n+}| + r - 1,$$

$$|V| = |Q| - |P_{k+}| - 1,$$

$$|H| = |R| + |V| + 1.$$
(8)

In accordance with the established form of the controlled plant, as defined by equation (5), we define the numerator polynomials of the specified transfer function of the controlled plant as follows:

$$P_{n+}(p) = 1, P_{k+}(p) = 1, P_{-}(p) = 1,$$
 (9)

and the polynomial expressions of the denominator of the specified transfer function of the controlled plant:

$$Q_{n+}(p) = 1, Q_{k+}(p) = (Tp+1),$$

$$Q_{-}(p) = (T_{2}p+1) \cdot (T_{3}p+1), s = 0.$$
(10)

We determine the degrees of the numerator and denominator polynomials of the controlled plant transfer function and its components, as defined by equations (9) and (10):

$$|P| = 0, |P_{k+}| = 0, |P_{n+}| = 0, |P_{-}| = 0,$$

 $|Q| = 3, |Q_{k+}| = 1, |Q_{n+}| = 0, |Q_{-}| = 2, s = 0.$
(11)

Improvement in the accuracy of control actions and the mitigation of disturbance torque effects in the automatic control system is achieved through the use of astatism-based regulators. Their implementation significantly enhances the control characteristics, particularly when an astatism regulator is applied to a static controlled plant. Accordingly, in the design of the current regulator, the corresponding astatism order r=1 is taken into account.

The value of expression (8) is calculated based on computations from (11):

$$|R| = |Q_{-}| + |Q_{n+}| + r - 1 = 2,$$

$$|V| = |Q| - |P_{k+}| - 1 = 2,$$

$$|H| = |R| + |V| + 1 = 5.$$
(12)

Let us denote $\tilde{R}(p)$, $\tilde{V}(p)$, $\tilde{H}(p)$ the corresponding polynomials with their degree reduced by one, which allows obtaining lower-order polynomials and thereby simplifies the implementation and tuning of the system. Using this approach, the geometric mean root of the characteristic polynomial H(p) becomes uniquely subordinate to the system's dynamic characteristics:

$$\omega_0 = \frac{1}{T_{-}},\tag{13}$$

where T_{st} — equivalent small time constant of the closed-loop current control system.

Considering (12), the following expression applies:

$$\begin{vmatrix} \tilde{R} \\ = |R| - 1 = 1, \\ |\tilde{V}| = |V| - 1 = 1, \\ |\tilde{H}| = |H| - 1 = 4. \end{vmatrix}$$
 (14)

Let the polynomials have the following complete form:

$$\tilde{R}(p) = r_i p + r_{i-1} p^{i-1} + \dots + r_1 p + r_0,$$

$$\tilde{V}(p) = v_i p + v_{i-1} p^{i-1} + \dots + v_1 p + v_0,$$
(15)

where i and j are the highest degrees of the corresponding polynomials.

Using relations (9) — (12), equation (7) can be rewritten in expanded form:

$$(r_1p + r_0) + (v_1p + v_0)(T_2p + 1)(T_3p + 1)p =$$

$$= \alpha_4 T_0^4 p^4 + \alpha_3 T_0^3 p^3 + \alpha_2 T_0^2 p^2 + \alpha_1 T_0 p + \alpha_0,$$
(16)

where α_0 , α_1 , α_2 , α_3 , α_4 , α_5 — the coefficients of the polynomial H(p) (for the fourth-order case, they are calculated and presented in Table 1).

Table 1. Coefficients of the characteristic polynomial distribution for the fourth-order current control loop H(n)

100p 11(p).							
Forms of stand- ard coefficient expressions	$\alpha_{_0}$	$\alpha_{_1}$	α_2	α_3	$\alpha_{_4}$		
Integral quality index I ₃	1	2.7	3.4	2.1	1		
Newton's binomial distribution	1	4	6	4	1		
Bessel distribu- tion	105	105	45	10	1		
Butterworth distribution	1	2.61	3.41	2.61	1		
Chebyshev distribution	0.38	1.03	1.72	1.20	1		
Integral quality index I ₂	1	2	3	1	1		

To prevent overshoot in the current control loop during subsequent regulator calculations, the distribution of the characteristic polynomial

coefficients is performed using the Butterworth method.

Let us determine the coefficients of the polynomials $\tilde{R}(p)$, $\tilde{V}(p)$. As a result, analytical expressions are obtained for calculating the transfer function of the current regulator of the automatic control system of the traction asynchronous motor of a transport dieselgenerator power plant:

$$v_1 = \frac{\alpha_4}{T_2 T_3 \omega_0^4} \tag{17}$$

$$v_0^{(1)} = \frac{\alpha_2}{\omega_0^2} - v_1$$

$$T_2 + T_2$$
(18)

$$v_0^{(2)} = \frac{\frac{\alpha_3}{\omega_0^3} - v_1(T_2 + T_3)}{T_2 T_3}$$
 (19)

$$r_1 = \frac{\alpha_1}{\omega_0} - v_0 \tag{20}$$

$$r_0 = \frac{\alpha_0}{\omega_0^0}. (21)$$

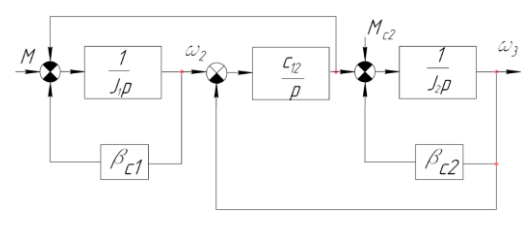
Using expressions (18) and (19), the values of the geometric mean root are determined under the condition that the right-hand sides of the formulas are equal, which is required for the synthesis of the regulator.

It is necessary, however, that at least one solution of this formula be a positive real number, as this determines the feasibility of physically implementing the regulator.

The transfer function of the resulting current regulator is defined as follows:

$$W_{cr}(p) = \frac{(Tp+1)(r_1p+r_0)}{(v_1p+v_0)pk}.$$
 (22)

When analyzing dynamic processes in the electric drive, it is acceptable to represent the asynchronous motor and the mechanical components of the traction drive as a lumped-parameter system. In this case, the drive system, consisting of the asynchronous motor and a specified mechanical component with elastic couplings, can be represented, for transient analysis, as a two-mass electromechanical system, as shown in Fig. 3.



M — electromagnetic torque of the motor;

 J_1 — rotor moment of inertia;

 J_2 — equivalent total moment of inertia of the mechanical components of the drive system;

 C_{12} — equivalent shaft-referred total stiffness coefficient between the drive system elements;

 β_{c1} — magnitude of the stiffness of the asynchronous motor's mechanical characteristic;

 β_{c2} — viscous friction coefficient;

 ω_2 — rotor angular velocity;

 ω_3 — angular velocity;

 M_{c2} — static load torque.

Fig. 3. Structural diagram of the two-mass electromechanical system.

To analyze the general properties of the system, let us write the mathematical model of the induction motor in a rotating orthogonal coordinate system with angular velocity, oriented along the *x*-axis by the rotor flux linkage vector.

The motor equations take the following form (23) [42, 43]:

$$\begin{cases} u_{sx} = R_s i_{sx} + \sigma X_s D i_{sx} + \\ + k_r D \psi_r - \omega_{\psi_r} \sigma X_s D i_{sy}; \\ u_{sy} = R_s i_{sy} + \sigma X_s D i_{sy} + \\ + \omega_{\psi_r} (\sigma X_s D i_{sx} + k_r \psi_r); \\ 0 = \psi_r + T_r D \psi_r - k_r R_r T_r i_{sx}; \\ 0 = -k_r R_r T_r i_{sy} + (\omega_{\psi_r} - \omega_2) \psi_r; \\ M = k_r \psi_r i_{sy}; \\ M = M_c + J_1 D \omega_2. \end{cases}$$
(23)

In this case, the following system of notations is used: the indices "s" and "r" denote the belonging of a variable to the stator or rotor, respectively; the indices "x", "y" indicate the projection of the vector onto the corresponding axis in the rotating coordinate system (x,y); L_M — the equivalent mutual inductance of rotor and stator; Xs — the reactance of the stator winding; u,i,ψ,R,L — voltage, current, flux linkage, resistance, and self-inductance, respectively; z — the number of pole pairs; Mc — the load

(resisting) torque; T — time constant; D — operator of differentiation with respect to time.

In Fig. 4, the block diagram of the induction motor corresponding to equations (23) is shown,

taking into account the variable value of the magnetizing component of the stator current i_{sx} , and accordingly, the variable rotor flux linkage.

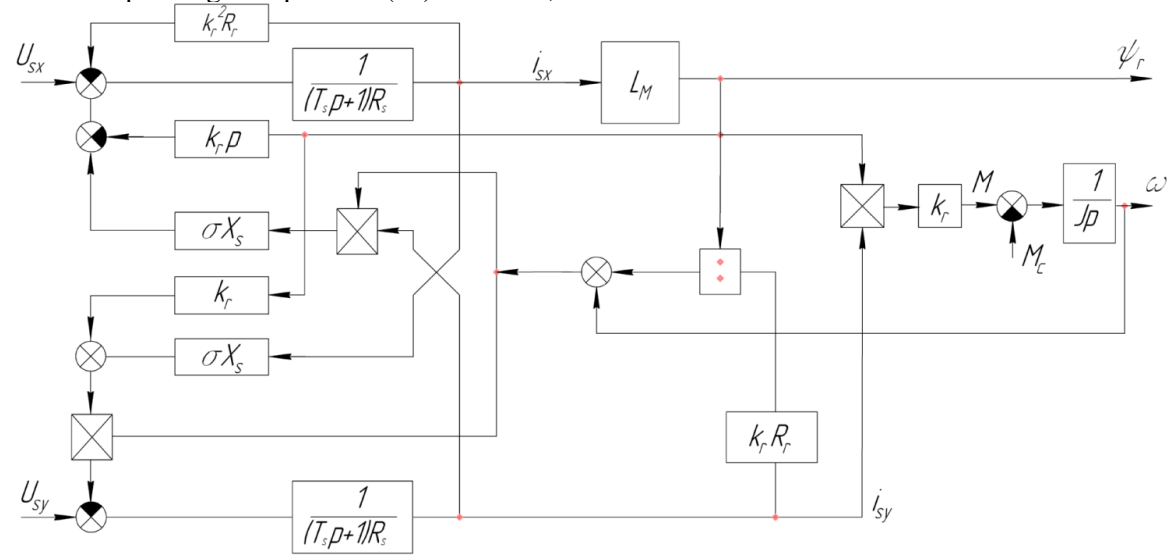


Fig. 4. Block diagram of the induction motor.

In (1), the following formulas are adopted for determining the leakage coefficient and the rotor time constant, respectively:

$$\sigma = 1 - \frac{L_M^2}{L_s L_r}, \ T_r = \frac{L_r}{R_s} = \frac{L_M}{k_s R_s}.$$
 (24)

where k_r — rotor winding transformation ratio.

To implement the control system of the frequency converter, we define its key switching function, which equals unity when the corresponding power module of the converter is conducting and zero otherwise. In the case of operation with an induction motor and when using a voltage-source inverter topology with an isolated neutral point, the simplex switching method can be represented by the following expressions:

$$U_{AB} = \begin{cases} \pm U_d & \text{if} \quad S_1 \cdot S_4 \text{ or } S_2 \cdot S_3 = 1; \\ 0 & \text{if} \quad S_1 \cdot S_3 = 1 \text{ or } S_2 \cdot S_4 = 1; \end{cases}$$

$$U_{BC} = \begin{cases} \pm U_d & \text{if} \quad S_3 \cdot S_6 & \text{or } S_4 \cdot S_5 = 1; \\ 0 & \text{if} \quad S_3 \cdot S_5 = 1 & \text{or } S_4 \cdot S_6 = 1; \end{cases}$$
(25)

$$U_{CA} = \begin{cases} \pm U_d & \text{if} \quad S_5 \cdot S_2 \text{ or } S_6 \cdot S_1 = 1; \\ 0 & \text{if} \quad S_1 \cdot S_5 = 1 \text{ or } S_2 \cdot S_6 = 1. \end{cases}$$

An inadmissible condition occurs when

$$\begin{cases} S_1 \cdot S_2 = 1; \\ S_3 \cdot S_4 = 1; \\ S_5 \cdot S_6 = 1. \end{cases}$$
 (26)

An extended description of the switching sequence for the frequency converter keys can allow the parallel connection of two phases of the induction motor in series with the third phase. Meanwhile, the remaining two phases of the induction motor change their state only with respect to the common DC bus, meaning that

$$U_{AB} = \begin{cases} \pm U_{d}, & \text{if } S_{1} \cdot S_{4} \cdot S_{5} \text{ or } S_{2} \cdot S_{3} \cdot S_{6} = 1; \\ 0, & \text{if } S_{1} \cdot S_{5} = 1, S_{4} = 0 \text{ or } S_{1} \cdot S_{5} = 0, S_{4} = 1; \end{cases}$$

$$U_{BC} = \begin{cases} \pm U_{d}, & \text{if } S_{3} \cdot S_{5} \cdot S_{2} \text{ or } S_{4} \cdot S_{1} \cdot S_{6} = 1; \\ 0, & \text{if } S_{3} \cdot S_{5} = 1, S_{2} = 0 \text{ or } S_{3} \cdot S_{5} = 0, S_{2} = 1; \end{cases}$$

$$U_{CA} = \begin{cases} \pm U_{d}, & \text{if } S_{5} \cdot S_{2} \cdot S_{4} \text{ or } S_{6} \cdot S_{1} \cdot S_{3} = 1; \\ 0, & \text{if } S_{4} \cdot S_{2} = 1, S_{5} = 0 \text{ or } S_{2} \cdot S_{4} = 0, S_{5} = 1. \end{cases}$$

II. RESULTS AND DISCUSSION

Using the data for the Caterpillar 3516 transport diesel–generator power plant [44-46] (maximum power: 2500 kVA / 2000 kW; rated power: 2275 kVA / 1820 kW; generator type: Caterpillar 1844, 50 Hz), the transient responses (unit step response) of the synthesized current regulator (22) and the baseline current regulator of the power plant were obtained, as shown in

Fig. 5. The control plant parameters are listed in Table 2.

Table 2. Control plant parameters.

Control plant parameter		
Parameter	Value	
Rated power, kW	240	
Rated RMS phase stator voltage, V	665	
Rated RMS phase stator current, A	135	
Rated RMS rotor current, A	128	
Rated magnetizing current, A	36	
Starting phase current, A	300	
Rated current frequency, Hz	33.8	
Maximum stator voltage frequency,	95	
Hz	93	
Rated rotor speed, rpm	1000	
Rated absolute slip, %	2	
Rotor moment of inertia, kg·m ²	21	
Rated electromagnetic torque, N·m	2366	
Stator resistance, Ω	0.083	
Rotor resistance, Ω	0.068	
Rotor electromagnetic time	1.294	
constant, s	1.474	
Rated efficiency, %	93.7	

Values of time constants of the regulator is 0,0809 s and the controlled object is 1.294 s.

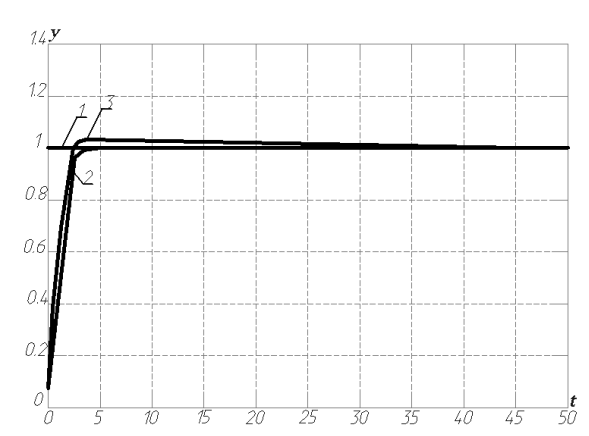


Fig. 5. Transient responses of the synthesized regulator (2) and the baseline current regulator (3) to a unit step command signal (1).

As shown in Fig. 5, the baseline regulator reaches the required command signal level faster, as it exhibits an overshoot of approximately 5%.

The synthesized regulator, however, shows no overshoot, which affects its stability and accuracy in achieving the desired value, since it does not incorporate overshoot coefficients (Vyshnegradsky coefficients). This influences the robustness of the transient response with respect to variations in the parameters of the control loops.

For instance, when the command signal reaches 0.92 of its set value (Fig. 6), the baseline regulator attains the target signal 0.71 times faster. Nevertheless, the response time of the synthesized regulator is within 10–13 ms, which is sufficient for the power system.

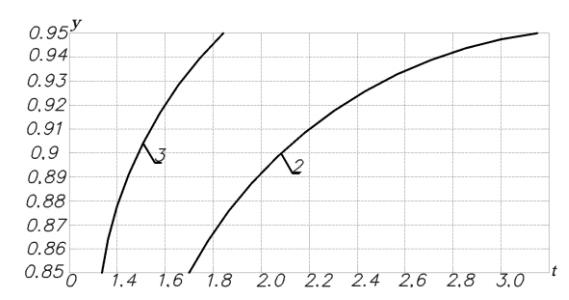


Fig. 6. Transient responses of the synthesized regulator (2) and the baseline current regulator (3) to a unit step command signal at 0.92 of the full command value.

The stator resistance of the induction motor varies during the warm-up process, as the temperature of the transport power system components can fluctuate between -45 °C and +65 °C. This results in a resistance change by a factor of 1.47, reflecting the impact of temperature variations on the system characteristics.

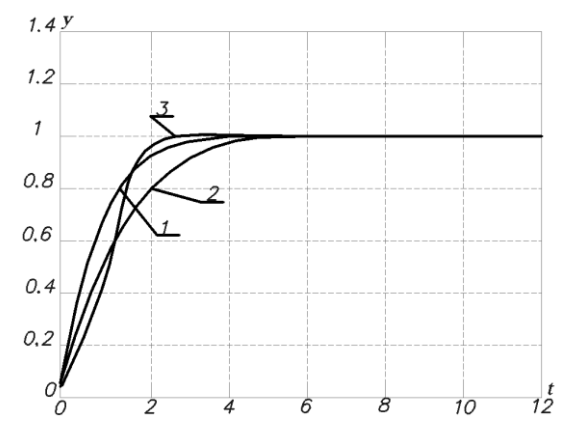


Fig. 7. Transient responses of the synthesized current regulator: with nominal stator resistance (1), with stator resistance decreased by a factor of 1.47 (3), and with stator resistance increased by a factor of 1.47 relative to nominal (2).

Automatic control systems synthesized using traditional approaches differ from those designed via the polynomial method in that they cannot maintain the required control quality when the stator resistance of the induction generator changes. To evaluate this, the stator resistance of the induction motor is decreased and increased by a factor of 1.47 relative to its nominal value. This allows assessment of how resistance variations affect the transient response of the synthesized current regulator, as shown in Fig. 7.

This test enables analysis of the regulator's stability and effectiveness under resistance variations.

For comparison, the performance of the baseline current regulator is also evaluated under the same conditions, with the stator resistance varied by a factor of 1.47 from its nominal value. This allows assessment of the baseline regulator's effectiveness under identical conditions and comparison of the results, as shown in Fig. 8.

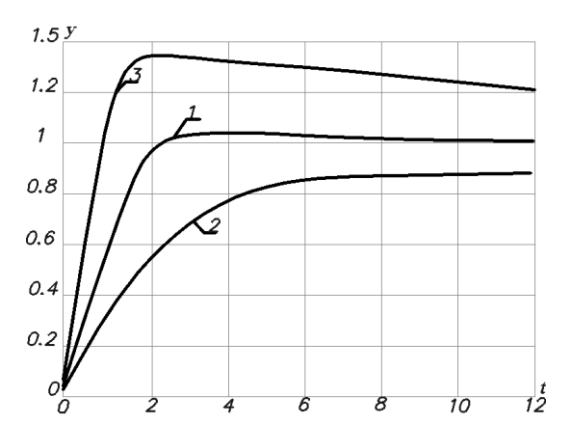


Fig. 8. Transient responses of the baseline current regulator: with nominal stator resistance (1), with stator resistance decreased by a factor of 1.47 (3), and with stator resistance increased by a factor of 1.47 relative to nominal (2).

According to Fig. 8, it can be concluded that the regulator synthesized using the subordinate control method exhibits unstable transient responses when the stator resistance of the induction motor is varied by a factor of 1.47 from its nominal value. An increase in stator resistance leads to a significant reduction in regulator speed, while a decrease in resistance results in overshoot of up to 46%. This indicates the instability of regulators synthesized using the subordinate control method under variations in the controlled plant parameters.

In contrast, the transient responses shown in Fig. 8 confirm the stability of the synthesized current regulator when the stator resistance of the induction motor is varied by the same factor of 1.47. This demonstrates its ability to maintain

stability even under variations in plant parameters.

As a result of experimental testing, oscillograms of the stator current i_s , the active component of the stator current i_{sy} , and the airgap flux linkage of the induction motor were obtained, as shown in Fig. 11. These oscillograms confirm the conclusions drawn from the simulation results.

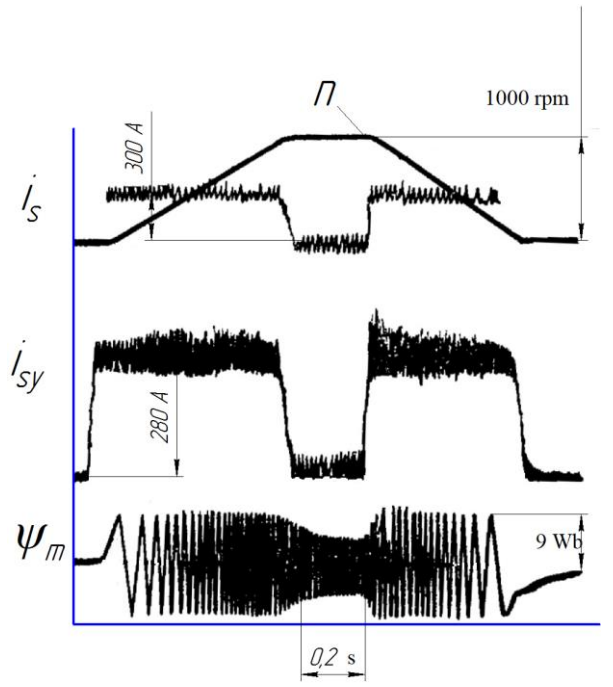


Fig. 11. Oscillograms from the experimental testing.

III. CONCLUSIONS

The fastest-acting control loop in the automatic control system of the traction induction motor in the transport diesel-generator power plant is the current control loop, which determines the dynamic properties of the entire system. Based on this, the block diagram of the induction motor current control loop and the closed-loop system control scheme were developed. The transfer function of synthesized regulator established. was reproducing satisfactory system errors and dynamic properties, and relationships were derived to determine the coefficients of the corresponding current regulator.

The obtained transient responses (unit step response) of the synthesized regulator and the baseline current regulator indicate that the regulator synthesized using the subordinate control method exhibits unstable transient behavior when the stator resistance is varied by a factor of 1.47 from its nominal value. Specifically, a decrease in stator resistance leads

to an overshoot of 44%, while an increase in resistance significantly reduces the regulator's response speed. This demonstrates the instability of subordinate-method regulators under variations in the plant parameters.

In contrast, the transient responses of the synthesized current regulator confirm the stability of its operation even when the stator resistance varies, demonstrating superior adaptability and effectiveness of the regulator under conditions of plant parameter variations.

References

- [1] Tarnapowicz D., German-Galkin S., Nerc A., Jaskiewicz M. Improving the Energy Efficiency of a Ship's Power Plant by Using an Autonomous Hybrid System with a PMSG. *Energies*, 2023, vol. 16, no. 7, pp. 3158.
- [2] Polakis M., Zachariadis P., Kat J.O. The Energy Efficiency Design Index (EEDI). In *Sustainable Shipping*; Springer: New York, NY, USA, 2019; pp. 93–135.
- [3] Cheng H., Chen H., Wang Q. An Integrated Drive Power Converter Topology for Plug-in Hybrid Electric Vehicle with G2V, V2G and V2H Functions. *Proceedings of the 2019 22nd International Conference on Electrical Machines and Systems (ICEMS)*, Harbin, China, 11–14 August 2019; pp. 1–6.
- [4] Jindo S., Kondo K., Kondo M., Yokouchi T. Power Generation Control Method of Parallel Resonant PMSG System for Series Hybrid Vehicle. *Proceedings of the 2022 International Power Electronics Conference (IPEC-Himeji 2022-ECCE Asia)*, Himeji, Japan, 15–19 May 2022; pp. 1878–1884
- [5] Chauhan A.K., Vakacharla V.R., Verma A.K., Singh S.K. Multiple PMSG fed Non-Inverting Buck-Boost Converter for HEVs. In Proceedings of the 2016 IEEE 6th International Conference on Power Systems (ICPS), New Delhi, India, 2016, pp. 1-6.
- [6] Wei J., Wang Y., Wen X., Li H., Zhang Y., Li K. A New Control Method for Microturbinegeneration based Series Hybrid Power System. In Proceedings of the 2019 22nd International Conference on Electrical Machines and Systems (ICEMS), Harbin, China, 2019, pp. 1-5.
- [7] Nayak S.K., Vinod H. Performance Study of Common DC Link Connected Wind and PV Hybrid System. In *Proceedings of the 2016 IEEE* 7th Power India International Conference (PIICON), Bikaner, India, 2016, pp. 1-5.
- [8] Giangrande P., Madonna V., Sala G., Kladas A., Gerada C., Galea M. Design and Testing of PMSM for Aerospace EMA Applications. In Proceedings of the IECON 2018—44th Annual Conference of the IEEE Industrial Electronics

- Society, Washington, DC, USA, 2018, pp. 2038-2043.
- [9] Ahmed J., Kumar L., Abbasi A.F., El Haj Assad M. Energy, Exergy, Environmental and Economic Analysis (4e) of a Solar Thermal System for Process Heating in Jamshoro, Pakistan. *Energies*, 2022, vol. 15, no. 22, pp. 8617.
- [10] Abdelaziz E.A., Saidur R., Mekhilef S. A review on energy saving strategies in industrial sector. Renew. Sustain. *Energy Rev.*, 2011, vol. 15, pp. 150-168.
- [11] Lamb W.F., Wiedmann T., Pongratz J., Andrew R., Crippa M., Olivier J.G., Wiedenhofer D., Mattioli G., Al Khourdajie A., House J., et al. A review of trends and drivers of greenhouse gas emissions by sector from 1990 to 2018. *Environ. Res. Lett.*, 2021, vol. 16, pp. 073005.
- [12] Maydison, Zhang H., Han N., Oh D., Jang J. Optimized Diesel-Battery Hybrid Electric Propulsion System for Fast Patrol Boats with Global Warming Potential Reduction. *Journal of Marine Science and Engineering*, 2025, vol. 13, no. 6, pp. 1071.
- [13] Pratama A.S., Prabowo A.R., Tuswan T., Adiputra R., Muhayat N., Cao B., Hadi S., Yaningsih I. Fast Patrol Boat Hull Design Concepts on Hydrodynamic Performances and Survivability Evaluation. J. *Appl. Eng. Sci.*, 2023, vol. 21, pp. 501-531.
- [14] Bouman E.A., Lindstad E., Rialland A.I., Strømman A.H. State-of-the-art technologies, measures, and potential for reducing GHG emissions from shipping—A review. *Transp. Res. Part D Transp. Environ.* 2017, vol. 52, 408–421.
- [15] Nitsenko V.V. Research on effect of differentialphase protection of busbars system with voltage of 110-750 kV. *Naukovyi Visnyk Natsionalnoho Hirnychoho Universytetu*. 2017, vol. 4, 72–79.
- [16] Kang L., Jiang D., Xia C., Xu Y., Sun K. Research and Analysis of Permanent Magnet Transmission System Controls on Diesel Railway Vehicles. *Electronics*, 2021, vol. 10, p. 173.
- [17] Lysechko V., Prokopenko V. Analysis of Current Approaches to Modernizing the Electric Power Scheme of Diesel Generator Transport. 2023 IEEE 4th KhPI Week on Advanced Technology (KhPIWeek), 2023, pp. 1–6.
- [18] Li W., Wang C., Pei H., Xu C., Lin G., Deng J., Jiang D., Huang Y. An Improved Energy Management Strategy of Diesel-Electric Hybrid Propulsion System Based on FNN-DP Strategy. *Electronics*, 2023, vol. 12, no. 3, p. 486. https://doi.org/10.3390/electronics12030486.
- [19] Konrad M., Jäger V., Pagenkopf J., Böhm M. Concept and Design of a Shunting Locomotive Equipped with a Hybridized Fuel Cell Hydrogen Powertrain. Proceedings of the 2021 Sixteenth International Conference on Ecological Vehicles

- and Renewable Energies (EVER), Monte-Carlo, Monaco, 5–7 May 2021; pp. 1–5.
- [20] Polater N., Tricoli P. Technical Review of Traction Drive Systems for Light Railways. *Energies*, 2022, vol. 15, p. 3187.
- [21] Viera Díaz R.I., Nuñez C., Visairo Cruz N., Segundo Ramírez J. A Polynomial Synthesis Approach to Design and Control an LCL-Filter-Based PWM Rectifier with Extended Functions Validated by SIL Simulations. *Energies*, 2023, vol. 16, no. 21, pp. 7382.
- [22] Vaideeswaran V., Veerakumar S., Sharmeela C., Bharathiraja M., Chandrasekaran P. Modelling of an Electric Vehicle Charging Station with PWM Rectifier to mitigate the Power Quality Issues. In *Proceedings of the Transportation Electrification Conference (ITEC-India)*, New Delhi, India, 2021, pp. 1-6.
- [23] Tawfeeq O.T., Ibrahim A.Y., Alabbawi A.A.M. Study of a Five-Level PWM Rectifier Fed DC Motor Drive. In *Proceedings of the 7th International Conference on Electrical and Electronics Engineering (ICEEE)*, Antalya, Turkey, 2020, pp. 126-129.
- [24] Rusek A., Shchur I., Lis M., Klatow K., Gastołek A., Sosnowski J. Mathematical model for analysis of dynamical states of a drive system containing rolling mill and roller table including the selected parameters of a rolling process. In 2015 16th International Scientific Conference on Electric Power Engineering (EPE), Kouty nad Desnou, Czech Republic, 2015, pp. 256-261.
- [25] Kuznetsov B., Bovdui I., Nikitina T., Kolomiets V., Kobylianskyi B. Multiobjective Parametric Synthesis of Robust Control by Rolling Mills Main Electric Drives. In 2020 IEEE Problems of Automated Electrodrive. Theory and Practice (PAEP), Kremenchuk, Ukraine, 2020, pp. 1-4.
- [26] Pan Z., Feng Y., Bu F., Zhang D., Lu Y., Yang Z. Anti-Impact Strategy of PMSM-Based Tension Control System for Flexible Rope Applications. In 2020 XI International Conference on Electrical Power Drive Systems (ICEPDS), 2020, pp. 1-6.
- [27] Moaveni B., Rashidi Fathabadi F., Molavi A. Fuzzy control system design for wheel slip prevention and tracking of desired speed profile in electric trains. *Asian J. Control* 2022, 24, 388–400.
- [28] Raluca-Cristina N., Ion V., Marian-Ștefan N., Sorin E. Investigation of Idle Running and Short-Circuit Performance Improvement for an Asynchronous Traction Motor. In *Proceedings of the 2019 International Conference on Electromechanical and Energy Systems* (SIELMEN), Craiova, Romania, 9–11 October 2019; IEEE: Piscataway, NJ, USA, 2019; pp. 1–6
- [29] Enache S., Vlad I., Enache M.A. Aspects Regarding the Optimization of Cross Geometry

- in Traction Asynchronous Motors Using the Theory of Nonlinear Circuits. *Energies* 2022, 15, 6648.
- [30] Costa C.A., Nied A., Nogueira F.G., de Azambuja Turqueti M., Rossa A.J., Dezuo T.J.M., Barra W. Robust Linear Parameter Varying Scalar Control Applied in *High Performance Induction Motor Drives. IEEE Trans. Ind. Electron.* 2020, 68, 10558–10568.
- [31] Hannan M.A., Ali J.A., Mohamed A., Hussain A. Optimization techniques to enhance the performance of induction motor drives: A review. *Renew. Sustain. Energy Rev.* 2018, 81, 1611–1626.
- [32] Lysechko V. P. The study of the cross-correlation properties of complex signals ensembles obtained by filtered frequency elements permutations. *Radio Electronics, Computer Science, Control*, 2022, no. 2, 15.
- [33] Mosaddegh H., Khoshhava M. A., Caron S. and Al-Haddad K. A Comprehensive Review of Restarting Strategies for Free Running Induction Motor Drives, 2024 International Conference on Electrical Machines (ICEM), Torino, Italy, 2024, pp. 1-6, doi: 10.1109/ICEM60801.2024.10700456.
- [34] Yin S. *et al.* Fast Restarting of Free-Running Induction Motors Under Speed-Sensorless Vector Control, in *IEEE Transactions on Industrial Electronics*, vol. 67, no. 7, pp. 6124-6134, July 2020, doi: 10.1109/TIE.2019.2934077.
- [35] Lee K., Ahmed S. and Lukic S. M. Universal Restart Strategy for High-Inertia Scalar-Controlled PMSM Drives, in *IEEE Transactions on Industry Applications*, vol. 52, no. 5, pp. 4001-4009, Sept.-Oct. 2016, doi: 10.1109/TIA.2016.2581764.
- [36] Elia N. and Mitter S. K. Stabilization of linear systems with limited information, in *IEEE Transactions on Automatic Control*, vol. 46, no. 9, pp. 1384-1400, Sept. 2001, doi: 10.1109/9.948466.
- [37] Wang Q., Duan Z. and Wang J. Distributed Optimal Consensus Control Algorithm for Continuous-Time Multi-Agent Systems, in *IEEE Transactions on Circuits and Systems II: Express Briefs*, vol. 67, no. 1, pp. 102-106, Jan. 2020, doi: 10.1109/TCSII.2019.2900758.
- [38] Ali M. N., Soliman M., Mahmoud K., Guerrero J. M., Lehtonen M. and Darwish M. M. F. Resilient Design of Robust Multi-Objectives PID Controllers for Automatic Voltage Regulators: D-Decomposition Approach, in *IEEE Access*, vol. 9, pp. 106589-106605, 2021, doi: 10.1109/ACCESS.2021.3100415.
- [39] Wu Y., Liang Q. and Hu J. Optimal Output Regulation for General Linear Systems via Adaptive Dynamic Programming, in *IEEE Transactions on Cybernetics*, vol. 52, no. 11, pp.

- 11916-11926, Nov. 2022, <u>doi:</u> 10.1109/TCYB.2021.3086223.
- [40] Pauwels E., Henrion D. and Lasserre J. -B. Inverse optimal control with polynomial optimization, *53rd IEEE Conference on Decision and Control*, Los Angeles, CA, USA, 2014, pp. 5581-5586, doi: 10.1109/CDC.2014.7040262.
- [41] Tadiparthi V., Bhattacharya R. Robust LQR for Uncertain Discrete-Time Systems using Polynomial Chaos, 2020 American Control Conference (ACC), Denver, CO, USA, 2020, pp. 4472-4477, doi: 10.23919/ACC45564.2020.9147831.
- [42] Bratkovska K., Makhlin P. Estimation of Optimization Approaches of the Energy Intensive Equipment's Power-Time Diagrams of Industrial Enterprises. 2022 IEEE 8th International Conference on ESS, 2022, pp. 277–281.

4250

- [43] Nitsenko V. Improvement implementation methods of relay busbars protection of switchgears. *Technical Electrodynamics*, 2017, (6), pp. 61–71.
- [44] Industrial Diesel Engines 3516. Available at: https://www.cat.com/en_US/products/new/power-systems/industrial/industrial-diesel-engines/18397893.html (accessed 29.06.2025).
- [45] Macari N. C., Richardson R. D. Operation of a Caterpillar 3516 Spark-Ignited Engine on Low-Btu Fuel. *J. Eng. Gas Turbines Power*, 1987, vol. 109, no. 4, pp. 443-447, doi: 10.1115/1.3240061.
- [46] Lam H., Richter M., Ashton G. A New Approach to Maximize the Potential of Reciprocating Engines Operating on Bio-Fuel Energy. *Paper No: ES2011-54496*, 2012, pp. 1149-1158. doi: 10.1115/ES2011-54496.

Author Information



Dmytro Oleksandrovych Kulagin, Doctor of Technical Sciences, Professor, Department of Industrial Power Supply, National University "Zaporizhzhia Polytechnic." Research interests: Dieselgenerator power plants, power conversion technologies, electrical machines and apparatus for transport systems. E-mail: kulagindo@gmail.com ORCID: 0000-0003-3610-



Ihor Zakharovych Maslov, Candidate of Technical Sciences, Associate Professor, Head of the Department of Marine Power Plants and Systems, Danube Institute, National University "Odessa Maritime Academy." Research interests: Power plants of transport systems. E-mail: maslovigor@i.ua ORCID: 0000-0003-1759-6077